

# Combined Wave and Current Interaction With a Rough Bottom

WILLIAM D. GRANT<sup>1</sup>

*Department of Ocean Engineering, Woods Hole Oceanographic Institution  
Woods Hole, Massachusetts 02543*

OLE SECHER MADSEN

*Department of Civil Engineering, Ralph M. Parsons Laboratory, Massachusetts Institute of Technology  
Cambridge, Massachusetts 02139*

An analytical theory is presented to describe the combined motion of waves and currents in the vicinity of a rough bottom and the associated boundary shear stress. Characteristic shear velocities are defined for the respective wave and current boundary layer regions by using a combined wave-current friction factor, and turbulent closure is accomplished by employing a time invariant turbulent eddy viscosity model which increases linearly with height above the seabed. The resulting linearized governing equations are solved for the wave and current kinematics both inside and outside the wave boundary layer region. For the current velocity profile above the wave boundary layer, the concept of an apparent bottom roughness is introduced, which depends on the physical bottom roughness as well as the wave characteristics. The net result is that the current above the wave boundary layer feels a larger resistance due to the presence of the wave. The wave-current friction factor and the apparent roughness are found as a function of the velocity of the current relative to the wave orbital velocity, the relative bottom roughness, and the angle between the currents and the waves. In the limiting case of a pure wave motion the predictions of the velocity profile and wave friction factor from the theory have been shown to give good agreement with experimental results. The reasonable nature of the concept of the apparent bottom roughness is demonstrated by comparison with field observations of very large bottom roughnesses by previous investigators. The implications of the behavior predicted by the model on sediment transport and shelf circulation models are discussed.

## INTRODUCTION

The shallow coastal zone along the inner continental shelf is an extremely dynamic region where the fluid motions associated with both surface waves and currents extend down to the sea floor and interact with the bottom sediments. The combined presence of surface waves and currents governs many physical processes of interest to oceanographers and engineers working in the coastal zone. The acquisition of the ability to model accurately the velocity distribution and bottom shear stress under combined waves and currents is essential to the study of sediment transport. Furthermore, understanding the interaction of combined wave and current flows with a rough bottom is critical to the study of the fluid dynamics and circulation on the inner continental shelf.

Only in recent years has recognition been given to the areal extent to which combined surface waves and currents play a significant role in sediment transport on the continental shelf. The importance of combined surface waves and currents on nearshore sediment transport has long been recognized. Surprisingly, for many years, only mean flows were considered to be important in deeper waters of 50–200 m. Field observations by *Komar et al.* [1972], *Butman et al.* [1977], and others indicate sediment resuspension due to waves in depths out to 200 m on the shelf. Such observations can be put on more quantitative grounds by studies of the initiation of sediment motion by *Madsen and Grant* [1975, 1976]. These studies point out the importance of accurate knowledge of the bottom shear stress in sediment transport under the action of waves and combined waves and currents.

It is worthwhile to consider briefly, from a qualitative view, the role of waves and currents in shelf sediment transport. Surface waves of 5–15 s start to feel the influence of the bottom in approximately 20–180 m of water, respectively. As these waves approach shallower water, the associated values of the near-bottom orbital velocities are of the same magnitude as those of the stronger coastal currents expected. However, the boundary shear stress associated with the wave motion may be an order of magnitude larger than the shear stress associated with a current of comparable magnitude. (Intuitively, this is easily pictured by considering the small scale of the wave boundary layer relative to that of the current boundary layer and comparing the respective vertical velocity gradients.) Thus waves are capable of entraining significant amounts of sediment from the seabed when a current of comparable magnitude may be too weak even to initiate sediment motion. On the other hand, waves are an inefficient transporting mechanism, and to the first order, no net transport is associated with the wave motion over a wave period. However, the simultaneous presence of even a weak current will cause a net transport.

The simple picture presented above of waves acting as a stirring mechanism making sediment available for transport by a weak current is a convenient conceptualization of combined waves and currents but is clearly an oversimplification of the process. In the immediate vicinity of the seabed the wave and current motions cannot be treated separately and then superposed. Rather, there is a nonlinear interaction between the two flows as a result of the presence of the bottom boundary. The fluid dynamics of the respective wave and current motions are altered from that expected for a pure wave motion or pure current because of the combined presence of each. The situation is further complicated, since the seabed is generally movable, and the fluid sediment interaction at the seabed results in the generation of bed forms which act as roughness elements to the flow. The presence of the bed forms modifies

<sup>1</sup>Formerly at the Department of Civil Engineering, Ralph M. Parsons Laboratory, Massachusetts Institute of Technology, Cambridge, Massachusetts 02139.

the flow in the vicinity of the bed, which in turn causes a modification of the bed forms. In most geophysical flows involving nonuniform, unsteady fluid motions, the process of bed form adjustment to the flow conditions is continually evolving. In addition, the resulting sediment transport can introduce flow stratification as well as cause an increased roughness. The process of fluid sediment interaction at the seabed provides an important link between the flow dynamics and sediment transport.

Unfortunately, our knowledge of the detailed structure of turbulent boundary layers over rough beds is quite poor. Laboratory work along the lines investigated by *Coleman et al.* [1977] is sorely needed. Even then, the extension of such laboratory studies to oscillatory flow over movable beds is likely to be quite far off. Nevertheless, even without such detailed knowledge of turbulent boundary layers, it is quite reasonable to expect that the large shear stress at the bed associated with the unsteady oscillatory wave motion will generate significant turbulence at the bed which can have a potential effect on the current motion in the case of combined wave and current flows.

The purpose of this paper is to present an analytical theory which treats the bottom friction under combined waves and currents in the presence of a rough bottom. The theory accounts for the nonlinear interaction between the two flows and gives the solutions for the wave and current kinematics both inside and outside the wave boundary layer as well as a solution for the wave-current friction factor used to define the bottom shear stress. The influence of the wave on the current is clearly shown, and for large waves relative to the current this influence is seen to be significant. The theory is compared qualitatively with field observations. In the limiting case of a pure wave motion, it has been compared quantitatively with laboratory data and found to give reasonable results [*Grant and Madsen*, 1978; *Grant*, 1977, 1978] (these three papers will subsequently be referred to as GM). The implications of the combined wave and current behavior predicted by the theory on sediment transport and coastal circulation models are discussed. Much of the formulation of the present work relies on the theoretical work of *Kajiura* [1964, 1968] and the experimental studies of *Jonsson* [1966] done on wave boundary layers. Surprisingly, the problem of combined waves and currents has received little attention either experimentally or analytically.

A theory for the combined interaction between waves and currents which is conceptually similar to this work was developed independently by *Smith* [1977] at the same time that the work presented here was being undertaken. However, significant differences exist between the two approaches. The present work treats the general problem of waves and currents at arbitrary angles, whereas *Smith's* [1977] work treats only the codirectional flow case. The treatments of the flow dynamics and the influence of the wave on the current differ between the two approaches. The definitions of the characteristic shear velocity used in the eddy viscosity models differ, and the present theory parameterizes the essential influence of the wave on the steady current above the wave boundary layer through an apparent increase in the roughness experienced by the current. In contrasting the two models, it is particularly important to keep in mind that the approach taken here in the development of a model for combined waves and currents tacitly assumes that the problem of interest is the interaction of waves and currents in a wave-dominated environment, whereas *Smith's* [1977] model approaches the problem from

the opposite end. Thus together the two models cover a wide range of conditions of interest on the shelf.

### PHYSICAL MODEL

The dominating physical feature that a model for combined waves and currents must deal with is the contrasting time scales associated with the fluid motions on the continental shelf: the slowly varying, essentially steady motion of the current, generally wind driven, tidal, or density driven and the unsteady oscillatory motion of the surface waves. Because of these contrasting time scales, the scales of two different boundary layer flows evolve. The current may be considered essentially as a fully developed flow with its associated boundary layer, i.e., the layer where the shear stress due to the current is considered to be significant, assumed to extend over most of the depth of flow in the absence of stratification. However, because of the short time scale of the wave the region in which the shear stress associated with the wave motion is significant, i.e., the oscillatory wave boundary layer, is confined to a relatively thin region close to the seabed. Thus in the immediate vicinity of the seabed the shear stress and turbulent intensities are due to the combined effect of both the wave and the current, which are coupled in a nonlinear fashion. In other words, when waves and currents exist jointly in a region, the shear stresses identified with the wave and with the current are altered because of the nature of the turbulence generated by the wave-current interaction and will be different, as was previously mentioned, from the shear stresses which would be experienced by either the wave or the current were they present by themselves. The end result is that the current in the region above the wave boundary layer, i.e., the potential flow region for the wave, experiences a shear stress which depends not only on the physical bottom roughness but also on the wave boundary layer characteristics. From the simple conceptualization above, it is evident that the flow kinematics and the flow dynamics are intricately related through the shear stress associated with the combined wave and current.

### THEORETICAL MODEL

The equation governing the fluid motion associated with a combined wave and current both inside and outside the wave boundary layer, assuming convective accelerations as well as Coriolis accelerations to be negligible, is given by

$$\frac{\partial \mathbf{u}}{\partial t} = -\frac{1}{\rho} \nabla p + \frac{\partial}{\partial z} \left( \frac{\tau}{\rho} \right) \quad (1)$$

where  $t$  is the time variable,  $\nabla$  is the vector operator

$$\nabla = \frac{\partial}{\partial x} \mathbf{i} + \frac{\partial}{\partial y} \mathbf{j} \quad (2)$$

$p$  is the pressure

$$p = p_w + p_c \quad (3)$$

and  $\mathbf{u}$  is the velocity vector

$$\mathbf{u} = \mathbf{u}_w + \mathbf{u}_c \quad (4)$$

The subscripts  $w$  and  $c$  in (3) and (4) indicate the components due to the wave (unsteady component) and the current (steady component), respectively. Convective acceleration terms of the form  $\mathbf{u} \partial \mathbf{u} / \partial x$  have been considered to be small in the governing equation; a simple scaling of (1) indicates that the analysis presented here is expected to be valid for values of the current of the same order of magnitude as the wave orbital speed.

To obtain an analytical solution to the system of equations (1)–(4), we relate the turbulent shear stress term to the flow kinematics through the use of a turbulent eddy viscosity  $\epsilon$ . For steady unidirectional flow the assumption is often made that, close to the boundary, the eddy viscosity varies linearly with distance from the sheared boundary, i.e.,

$$\epsilon = \kappa u_* z \tag{5}$$

where  $\kappa$  is Von Karman’s constant ( $\kappa = 0.4$  for clear water),  $z$  is the vertical coordinate measured positively upward from the boundary, and  $u_* = (\tau/\rho)^{1/2}$  is a characteristic shear velocity representing the turbulence level in the flow. The concept of a linearly varying eddy viscosity is similar to the concept of Prandtl’s mixing length hypothesis and results in the experimentally observed logarithmic velocity profile in the region adjacent to the sheared boundary. Clearly, when multiple length scales are involved, the mixing length hypothesis loses much of its meaning, and, for similar reasons, the same must be true of the eddy viscosity concept. However, judicious choice of the characteristic shear velocity for each length scale may be used to overcome this problem. It is also important to note that in steady unidirectional flow the velocity profile in the immediate vicinity of the bed shows little sensitivity to the choice of either a linearly varying eddy viscosity or a more physically pleasing form such as a parabolic distribution. Since the primary concern here is with the flow close to the bed, the simpler linearly varying form will be used.

Using the eddy viscosity concept discussed above, the stress divergence in (1) may be expressed as a linear function of the velocity. Thus

$$\frac{\partial}{\partial z} \left( \frac{\tau}{\rho} \right) = \frac{\partial}{\partial z} \left( \epsilon \frac{\partial u}{\partial z} \right) \tag{6}$$

Representing the stress divergence term by (6) and substituting (2), (3), and (4) into (1), the governing equation becomes

$$\frac{\partial \mathbf{u}_w}{\partial t} = -\frac{1}{\rho} \nabla p_c - \frac{1}{\rho} \nabla p_w + \frac{\partial}{\partial z} \epsilon \frac{\partial \mathbf{u}_w}{\partial z} + \frac{\partial}{\partial z} \epsilon \frac{\partial \mathbf{u}_c}{\partial z} \tag{7}$$

From (7), which is linear, two equations are obtained, one governing the steady current motion and the other governing the unsteady wave motion.

The physical model discussed previously indicated that two distinct boundary layer regions existed for the combined wave and current flow. To be consistent with this physical model, the eddy viscosity used in (7) must reflect the characteristics of the flow in each region. Thus before proceeding with the theoretical model we must first address the problem of the appropriate scaling for the eddy viscosity in (7). To do this, we define the relationship between the flow dynamics (shear stress) and the flow kinematics (velocity field) in the immediate vicinity of the seabed. Such a definition is fundamental to a model of combined waves and currents.

DEFINITIONS

For turbulent flows associated with a pure wave motion as well as in unidirectional steady flow a quadratic drag law is generally adopted to model the bottom friction [e.g., Jonsson, 1966; Kajiura, 1964]. Thus a reasonable definition relating the instantaneous boundary shear stress  $\tau_b$  to the combined wave and current velocity field  $\mathbf{u}_{cw}$  is taken as

$$\tau_b = \frac{1}{2} \rho f_{cw} (u^2 + v^2) \left[ \frac{u}{(u^2 + v^2)^{1/2}}, \frac{v}{(u^2 + v^2)^{1/2}} \right] \tag{8}$$

where  $\rho$  is the fluid density,  $f_{cw}$  is a friction factor associated with the combined wave and current flow, and  $u$  and  $v$  are the  $x$  and  $y$  components, respectively, of the horizontal velocity ( $[u^2 + v^2]^{1/2} = |\mathbf{u}_{cw}|$ ). Adopting the convention that the  $x$  axis is always in the direction of wave propagation,  $u$  and  $v$  may be expressed as

$$u = (\sin \theta + (|\mathbf{u}_a|/|\mathbf{u}_b|) \cos \phi_c) |\mathbf{u}_b| \equiv g_x |\mathbf{u}_b| \tag{9}$$

and

$$v = [(|\mathbf{u}_a|/|\mathbf{u}_b|) \sin \phi_c] |\mathbf{u}_b| \equiv g_y |\mathbf{u}_b| \tag{10}$$

where  $|\mathbf{u}_a|$  is the magnitude of the steady current velocity vector at a height  $a$  above the bottom;  $\phi_c$  is the angle made by  $\mathbf{u}_a$  with the direction of wave propagation;  $|\mathbf{u}_b|$  is the maximum near-bottom orbital velocity from linear wave theory, i.e., in the potential flow region above the wave boundary layer; and  $\theta$  is the phase angle ( $\theta = \omega t$ ) associated with a fluid particle undergoing simple harmonic motion of radian frequency  $\omega$ . Since we will only be concerned with linear wave theory in the following developments,  $\phi_c$  only needs to be defined from  $0^\circ$  to  $90^\circ$ .

The current velocity  $\mathbf{u}_a$  used in the definition of the bottom shear stress under the combined wave motion and steady current is treated as an unknown in the model developed here. Since the bed shear stress will depend upon the relative magnitudes of the steady and unsteady components of the flow as well as the bottom roughness, which are all related in a complex nonlinear fashion, it is not clear from a physical viewpoint what the appropriate current is for  $\mathbf{u}_a$ . Thus  $\mathbf{u}_a$  is left to float and is determined as part of the solution to the wave-current problem as a function of the relative wave and current flows (it should be remembered that these are modified because of their interaction) as well as the physical bottom roughness.

The preceding definition of the shear stress has disregarded a possible phase shift between the maximum value of the reference velocity  $(u^2 + v^2)^{1/2}$  and the maximum shear stress. For the purpose of introduction here, this is not critical and will be treated subsequently.

The above definition, given by (8), can now be used to define characteristic shear velocities associated with the fluid motions in the respective boundary layer regions. In the region above the wave boundary layer the shear stress is associated only with the steady current, since the wave motion is assumed to be described by potential theory. With the time dependent boundary shear stress given by (8) the steady current in this upper region is affected by the time average shear stress, the magnitude of which is defined as

$$|\tau_c| = \frac{1}{2} \rho f_{cw} |\mathbf{u}_b|^2 \left( \frac{1}{2\pi} \right) \left\{ \left[ \int_{-\theta_*}^{\pi+\theta_*} (g_x^4 + g_x^2 g_y^2)^{1/2} d\theta - \int_{\pi+\theta_*}^{2\pi-\theta_*} (g_x^4 + g_x^2 g_y^2)^{1/2} d\theta \right]^2 + \left[ \int_0^{2\pi} (g_y^4 + g_x^2 g_y^2)^{1/2} d\theta \right]^2 \right\}^{1/2} \tag{11}$$

where direction has been taken into account in the time-averaging process, reflecting the concept that the current has a memory, and  $g_x$  and  $g_y$  are given in (9) and (10), respectively. The  $x$  component of the shear stress given by (8) is positive over the interval  $-\theta_*$  to  $\pi + \theta_*$  and negative over the interval  $\pi + \theta_*$  to  $2\pi - \theta_*$  with

$$\theta_* = \sin^{-1} [(|\mathbf{u}_a|/|\mathbf{u}_b|) \cos \phi_c] \tag{12}$$

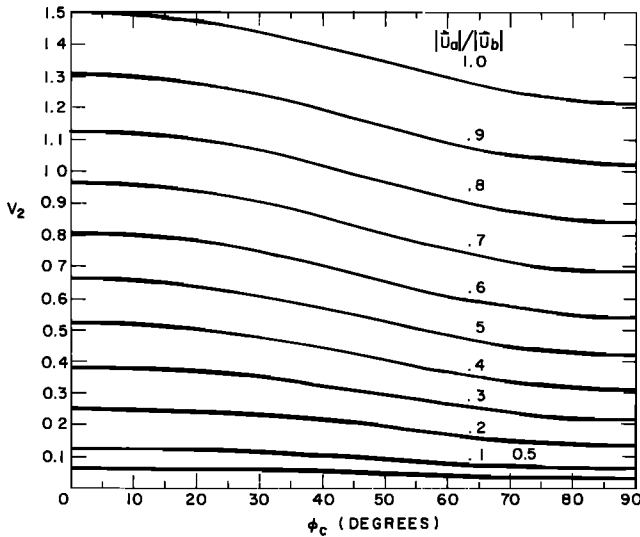


Fig. 1. Numerical solution to  $V_2$  given by (14). Note that for  $|u_a|/|u_b| > 1/\cos \phi_c$ ,  $\theta_* = \pi/2$ .

We note that the  $\theta_*$  has real solutions only when

$$|u_a|/|u_b| \leq 1/\cos \phi_c \tag{13}$$

Denoting the terms in braces in (11) as

$$V_2 = \left( \frac{1}{2\pi} \right) \left\{ \left[ \int_{-\theta_*}^{\pi+\theta_*} (g_x^4 + g_x^2 g_y^2)^{1/2} d\theta - \int_{\pi+\theta_*}^{2\pi-\theta_*} (g_x^4 + g_x^2 g_y^2)^{1/2} d\theta \right]^2 + \left[ \int_0^{2\pi} (g_y^4 + g_x^2 g_y^2)^{1/2} d\theta \right]^2 \right\}^{1/2} \tag{14}$$

the magnitude of the shear velocity  $|u_{*c}|$  based on the time-averaged shear stress can be found from (11) as

$$\rho^{-1} |\tau_c| = |u_{*c}|^2 = \frac{1}{2} f_{cw} V_2 |u_b|^2 \tag{15}$$

The integrals defined in (14) may be expressed in terms of elliptical integrals, and the results of a numerical solution are given in Figure 1. A convenient approximation for  $V_2$  for small currents relative to the wave motion is

$$V_2 = (2/\pi) (|u_a|/|u_b|) [4 - 3 \sin^2 \phi_c]^{1/2} \tag{16}$$

The direction associated with the mean stress vector whose magnitude is given by (15) will act at an angle  $\phi_c$  with the direction of wave propagation such that the force driving the 'steady' current will be balanced. This direction is, of course, the same as the direction of the steady current above the wave boundary layer. The direction of the mean stress is not in general the same as the direction of the steady current inside the wave layer,  $\phi_c$ . The adoption of a nonlinear relationship, given by (8), between the bottom shear stress and the velocity causes the direction of the current vector  $u_a$  to diverge from the direction of the average shear stress.

The angle  $\bar{\phi}_c$  associated with the mean stress may be expressed as

$$\bar{\phi}_c = \tan^{-1} \left\{ \left[ \int_0^{2\pi} (g_y^4 + g_x^2 g_y^2)^{1/2} d\theta \right] \cdot \left[ \int_{-\theta_*}^{\pi+\theta_*} (g_x^4 + g_x^2 g_y^2)^{1/2} d\theta \right] \right\}$$

$$- \int_{\pi+\theta_*}^{2\pi-\theta_*} (g_x^4 + g_x^2 g_y^2)^{1/2} d\theta \Big]^{-1} \tag{17}$$

and is thus seen to be explicitly related to the direction of the velocity vector  $u_a$ . For small currents relative to the wave ( $|u_a|/|u_b| \lesssim 0.2$ ), (17) simplifies to

$$\tan \bar{\phi}_c = \frac{1}{2} \tan \phi_c \tag{18}$$

Figure 2 shows graphically the relationships expressed by (17) and (18).

Equation (8) represents the nonlinear interaction between an unsteady wave motion and a steady current motion, each of which acts to enhance the other. As a result the formulation in (8) is not equivalent to adding the shear stress due to a pure wave to the shear stress due to a pure current. Primarily, this nonlinear interaction is reflected through the wave-current friction factor. However, to treat the mathematical aspects of the problem, the shear stress is partitioned into two parts: one part associated with the steady component of the enhanced motion given by (15) and the other part associated with the enhanced unsteady motion which is treated below. Above the wave boundary layer the partitioning is straightforward, since only the current shear stress must be dealt with; in this region the driving force, current, and shear stress all act in the same direction.

The process of partitioning is not so simple inside the wave boundary layer, where the shear stress is associated with both the wave and the current motions. The average shear stress divergence must still balance the force driving the steady current within the wave boundary layer. As a result the nonlinear relationship given in (8) requires the current velocity  $u_a$  to form a greater angle with the  $x$  axis. Physically, the turning of the reference current may be thought of as being caused by the dominating influence of the waves, a contention which is supported by the behavior of  $\phi_c$  and  $\bar{\phi}_c$  as a function of  $|u_a|/|u_b|$  in Figure 2.

The characteristic shear velocity associated with the combined wave and current motion inside the wave boundary layer

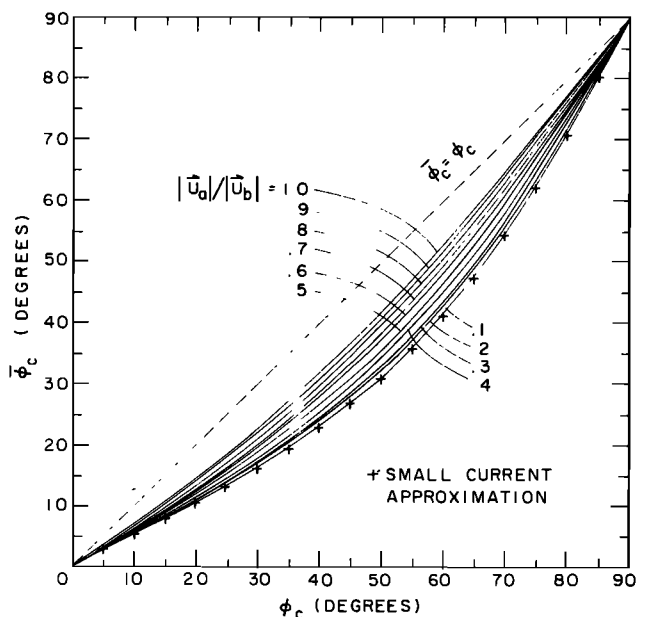


Fig. 2. Relationship between reference angle  $\phi_c$  and current direction  $\bar{\phi}_c$  outside the wave boundary layer (17) and for small  $|u_a|/|u_b|$ , (18).

must be defined next. The magnitude of the maximum boundary shear stress due to the combined wave and current is found, using (8), as

$$|\tau_{b,\max}| = \frac{1}{2} f_{cw} \rho \alpha |\mathbf{u}_b|^2 \quad (19)$$

where

$$\alpha = 1 + (|\mathbf{u}_a|/|\mathbf{u}_b|)^2 + 2(|\mathbf{u}_a|/|\mathbf{u}_b|) \cos \phi_c \quad (20)$$

We then define the characteristic turbulent intensity in the wave boundary layer region based on (19) as

$$|\mathbf{u}_{*cw}| = (|\tau_{b,\max}|/\rho)^{1/2} = (\frac{1}{2} f_{cw} \alpha)^{1/2} |\mathbf{u}_b| \quad (21)$$

Note that  $|\mathbf{u}_{*cw}|$  reflects the nonlinear aspects of the wave current interaction.

Using the definitions of the characteristic turbulent intensities above the wave boundary layer and inside the wave boundary layer, given by the square root of (15) and by (21), respectively, it follows that the appropriate forms of the eddy viscosity in each region are

$$\epsilon_c = \kappa |\mathbf{u}_{*c}| z \quad z > \delta_w \quad (22)$$

and

$$\epsilon_{cw} = \kappa |\mathbf{u}_{*cw}| z \quad z < \delta_w \quad (23)$$

respectively, where  $\delta_w$  is the wave boundary layer thickness.

The form of the eddy viscosity given by (23) is time invariant. At the seabed the turbulent intensities are expected to respond rapidly to the changing flow conditions so that the instantaneous value of the shear stress is required. Unfortunately, the use of a time-varying eddy viscosity results in a governing equation which cannot be solved analytically. The use of a time invariant eddy viscosity based on the maximum shear velocity will overestimate the eddy viscosity only during low-velocity parts of the flow cycle. Furthermore, in the model presented here, the form of the eddy viscosity given by (23) will be used only to solve for the kinematics of the problem, that is, to define the maximum velocity profile. The time variation will be included in the treatment of the dynamics.

Experimental studies using laboratory waves discussed by *Horikawa and Watanabe* [1968] show that although the instantaneous value of the eddy viscosity varied periodically as expected, the mean value of the eddy viscosity is adequately represented by a continuous function of  $z$ . In the region close to the sheared boundary the function is reasonably approximated by a linear variation in  $z$ . An extensive treatment of a pure wave motion using the assumption of an eddy viscosity of the form given by (23), i.e., with the characteristic shear velocity based on the maximum value of the boundary shear stress, is given by GM. These results yield good predictions of the experimentally measured velocity profiles in *Jonsson and Carlsson's* [1976] study of oscillatory boundary layers.

By using the definitions given by (22) and (23), (7) can now be solved for the wave and current velocities in each boundary layer region. Before presenting and discussing the solutions it is important to emphasize that the definitions and concepts behind the theoretical model presented here are based upon analogies drawn with both unidirectional flows and unsteady oscillatory flow. The extension of these concepts to combined waves and currents is admittedly by conjecture. However, significant support for the approach is drawn from the reasonable nature of the results to be presented. Also, the successful use of the time independent eddy viscosity in an extensive treatment of the flow kinematics associated with a pure oscillatory

motion by GM lends further support to the approach taken here.

#### SOLUTION FOR THE WAVE MOTION

Outside the wave boundary layer the wave motion is governed by

$$\frac{\partial \mathbf{u}_w}{\partial t} = -\frac{1}{\rho} \nabla p_w + \frac{\partial}{\partial z} \left( \kappa |\mathbf{u}_{*c}| z \frac{\partial \mathbf{u}_w}{\partial z} \right) \quad z > \delta_w \quad (24)$$

where (22) has been used to express the eddy viscosity term. Since  $|\mathbf{u}_{*c}|$  is much less than the wave phase speed, the internal dissipation of wave energy represented by the gradient stress term on the right-hand side of (24) may be neglected, and (24) becomes

$$\frac{\partial \mathbf{u}_w}{\partial t} = -\frac{1}{\rho} \nabla p_w \quad z > \delta_w \quad (25)$$

which is the familiar Euler equation. Appropriate linearization of the boundary conditions and application of the principle of conservation of mass along with the assumption of irrotational flow leads to the well-known solution for linear wave theory. This is given in any standard text [e.g., *Madsen*, 1976] and will not be discussed further here. This solution describes the simple harmonic motion of a fluid particle which, at the wave boundary layer interface, oscillates in a path nearly parallel to the bed with a velocity  $\mathbf{u}_\infty$ . Introducing complex notation,

$$\mathbf{u}_\infty = |\mathbf{u}_b| e^{i\omega t}$$

where  $i = (-1)^{1/2}$  and, in the usage here, the physical solution is given by the imaginary part.

Inside the wave boundary layer, the wave motion is governed by

$$\frac{\partial \mathbf{u}_w}{\partial t} = -\frac{1}{\rho} \nabla p_w + \frac{\partial}{\partial z} \left( \kappa |\mathbf{u}_{*cw}| z \frac{\partial \mathbf{u}_w}{\partial z} \right) \quad z < \delta_w \quad (26)$$

where the influence of the current motion on the wave is clearly seen through the  $|\mathbf{u}_{*cw}|$  term. Since the vertical velocities are negligible in the immediate vicinity of the bed, the pressure term in (26) may be expressed as

$$\partial \mathbf{u}_\infty / \partial t = -\frac{1}{\rho} \nabla p_w \quad (27)$$

Introducing (27) into (26) and letting  $(\mathbf{u}_w - \mathbf{u}_\infty) = \mathbf{w} = |\mathbf{w}| e^{i\omega t}$ , (26) becomes

$$\frac{\partial}{\partial z} \left( \frac{\kappa |\mathbf{u}_{*cw}|}{\omega} z \frac{\partial |\mathbf{w}|}{\partial z} \right) - i |\mathbf{w}| = 0 \quad (28)$$

where only the imaginary part of the solution is retained. (The vector notation has been deleted on the wave velocity, since by definition it is always along the  $x$  axis.) The length scale  $l$  of the region where a significant deviation of the boundary layer velocity from the free stream velocity can be expected is identified from (28) as

$$l = \kappa |\mathbf{u}_{*cw}| / \omega \quad (29)$$

Thus we see that the thickness of the wave boundary is limited by frequency. Using a change of variable,  $\zeta = z/l$ , (29) becomes

$$\frac{\partial}{\partial \zeta} \left( \zeta \frac{\partial |\mathbf{w}|}{\partial \zeta} \right) + i^3 |\mathbf{w}| = 0 \quad (30)$$

The no-slip requirement at the bed is taken in an analogous form to that used in fully rough turbulent unidirectional flow as

$$w \rightarrow -u_\infty \quad \text{at} \quad \zeta = \zeta_0 = k_b/30l \quad (31)$$

where  $k_b$  is the characteristic dimension of the physical bottom roughness. (More discussion of (31) is given below.) At the wave boundary layer interface the boundary layer velocity must approach the free stream velocity; hence we require as the second boundary condition

$$w \rightarrow 0 \quad \text{as} \quad \zeta \rightarrow \infty \quad (32)$$

The general solution to (30) [e.g., *Hildebrand*, 1965] may be conveniently written in terms of Kelvin functions of zeroth order as

$$w = A(\text{Ber } 2\zeta^{1/2} + i \text{Bei } 2\zeta^{1/2}) + B(\text{Ker } 2\zeta^{1/2} + i \text{Kei } 2\zeta^{1/2}) \quad (33)$$

Since *Ber* and *Bei* become exponentially large as  $\zeta \rightarrow \infty$  [*Abramowitz and Stegun*, 1972, Figure 9.10], (32) requires that  $A = 0$  in (33). Invoking the boundary condition expressed by (31) in (33) and setting  $A = 0$  yield for the second constant

$$B = \frac{-u_\infty}{\text{Ker } 2\zeta_0^{1/2} + i \text{Kei } 2\zeta_0^{1/2}} \quad (34)$$

The introduction of (34) in (33) gives the wave velocity within the wave boundary layer

$$u_w = \left[ 1 - \frac{\text{Ker } 2\zeta^{1/2} + i \text{Kei } 2\zeta^{1/2}}{\text{Ker } 2\zeta_0^{1/2} + i \text{Kei } 2\zeta_0^{1/2}} \right] u_\infty \quad (35)$$

From (35) the magnitude of the wave velocity inside the wave boundary layer can be found as well as the phase shift between  $u_w$  and the free stream velocity  $u_\infty$ . This is a straightforward exercise and is treated by GM. Close to the boundary, (35) may be approximated by a logarithmic profile using the small argument approximations for *Ker* and *Kei* (GM). Thus for  $\zeta \rightarrow 0$ ,

$$u_w = \left[ 1 + \frac{0.5}{(\text{Ker } 2\zeta_0^{1/2} + i \text{Kei } 2\zeta_0^{1/2})} \left( \ln \zeta + 1.154 + \frac{i\pi}{2} \right) \right] u_\infty \quad (36)$$

It is important to recall that the characteristic shear velocity  $|u_{*cw}|$  is implicitly related to  $u_w$  through the arguments of the *Ker* and *Kei* functions and carries with it the influence of the current. The influence of the boundary roughness is also reflected in the solution given by (35) or (36) by the dependence of  $\zeta_0$  on the physical bottom roughness  $k_b$ . This dependence is seen through (31). More will be said about the influence of the bed roughness on  $u_w$  in the discussion of the dynamics of the combined wave-current flow.

The length scale  $l$  of the region over which the shear stress associated with the waves is expected to be important was identified in (29). The wave boundary layer thickness may be conveniently defined in terms of  $l$ . Physically, this means the region where the boundary layer velocity approaches the free stream velocity, or in terms of (35),

$$\frac{\text{Ker } 2\zeta^{1/2} + i \text{Kei } 2\zeta^{1/2}}{\text{Ker } 2\zeta_0^{1/2} + i \text{Kei } 2\zeta_0^{1/2}} \rightarrow 0 \quad \text{as} \quad \zeta \rightarrow \infty \quad (37)$$

where  $\infty$  denotes the region of the 'free stream,' i.e., potential flow, velocity. Mathematically, this occurs for values of  $\zeta \sim 2$

to 4 or greater. No precise definition exists for the location of the upper boundary layer interface in terms of the boundary layer velocity as a fixed percentage of the free stream velocity (e.g., 98% as opposed to 99%), and to obtain the correct behavior in the limit of a pure wave, we may argue physically that

$$\delta_w = 2l \quad (38)$$

This definition is discussed in considerable detail by GM. However, the assumption of  $\delta_w = 2l$  or  $4l$  is not critical to the results of the model presented here.

#### SOLUTION FOR THE STEADY CURRENT

For the current motion outside the wave boundary layer, (7) and (22) yield the governing equation

$$-\frac{1}{\rho} \nabla p_c + \frac{\partial}{\partial z} \left( \kappa |u_{*c}| z \frac{\partial u_c}{\partial z} \right) = 0 \quad z > \delta_w \quad (39)$$

and for the current inside the wave boundary layer, (7) and (23) give

$$-\frac{1}{\rho} \nabla p_c + \frac{\partial}{\partial z} \left( \kappa |u_{*cw}| z \frac{\partial u_c}{\partial z} \right) = 0 \quad z < \delta_w \quad (40)$$

Since the scale of the wave boundary layer is small, the contribution of the pressure term in (40) may be disregarded. The region close to the boundary is assumed to be a region of constant stress, and (39) and (40) become

$$\kappa |u_{*c}| z \frac{\partial u_c}{\partial z} = u_{*c}^2 \quad z > \delta_w \quad (41)$$

and

$$\kappa |u_{*cw}| z \frac{\partial u_c}{\partial z} = u_{*c}^2 \quad z < \delta_w \quad (42)$$

respectively.

Inside the wave boundary layer the current motion is governed by (42), which may be integrated to yield the velocity profile for this region. The integration constant is evaluated subject to the no-slip boundary condition at the bed

$$u_c = 0 \quad \text{at} \quad z = z_0 = k_b/30 \quad (43)$$

The choice of location of the theoretical bottom at  $z = k_b/30$  is based on experimental results for steady, unidirectional rough turbulent flow [e.g., *Schlichting*, 1968]. This choice is made since, for combined waves and currents, the seabed will generally be expected to exhibit bed forms which would make the flow fully rough. For conditions other than fully rough flow the result can be generalized to  $z_0 = k_b/N$ , where  $N$  is a function of the roughness Reynolds number. Thus  $z_0$  can vary with the roughness length scale as well as with the bed shear stress. In the case of a movable bed subjected to a unidirectional flow, *Smith and McLean* [1977] have found that intense bed load transport causes large values of  $z_0$ . It is reasonable to expect that intense bed load transport may have an influence on  $z_0$  in unsteady oscillatory flow. However, the relationship between the roughness scale associated with the wave-formed ripples and the roughness scale associated with the bed load may be quite complex in oscillatory flow; the bed forms first grow and then decay to a flat bed as the bed shear stress increases, whereas the bed load transport continues to grow with bed shear stress. Our present understanding of the flow structure close to the bed in the presence of roughness elements and movable beds is not developed to the extent

where much will be gained from further speculation on the value of  $z_0$  in the simple model presented here.

Returning to our model and applying (43), the magnitude of the steady current velocity inside the wave boundary layer becomes

$$|u_c| = \frac{|u_{*c}|}{\kappa} \left( \frac{|u_{*c}|}{|u_{*cw}|} \right) \ln \frac{30z}{k_b} \quad z < \delta_w \quad (44)$$

The influence of the wave on the current is clearly seen through the term  $|u_{*c}|/|u_{*cw}|$ . By definition this term is always less than 1, and the presence of the wave motion tends to retard the current velocity over that expected for a pure current.

The solution for the current outside the wave boundary layer is obtained by integrating (41), which yields

$$|u_c| = \frac{|u_{*c}|}{\kappa} \ln z + c_0 \quad (45)$$

where  $c_0$  is an undetermined integration constant. In order to evaluate  $c_0$  we use the no-slip boundary condition at the seabed, as in the previous case. We argued previously that the total resistance felt by the flow reflects the turbulent intensity in the flow which is directly related to the hydrodynamic roughness. Then in a form analogous to (43) the law of the wall becomes

$$|u_c| = 0 \quad \text{at} \quad z = k_{bc}/30 \quad (46)$$

where the parameter  $k_{bc}$  is introduced as an apparent roughness which reflects the turbulence level at the seabed associated with the wave boundary layer as well as that associated with the physical bottom roughness. More discussion on the apparent roughness is given below, after we present the solution to (41). Using (46), the velocity profile for the steady current above the wave boundary layer is found from (45) as

$$|u_c| = \frac{|u_{*c}|}{\kappa} \ln \frac{30z}{k_{bc}} \quad z > \delta_w \quad (47)$$

It is clear from (47) that the major influence of the wave on the current is reflected through the apparent roughness parameter  $k_{bc}$ . (From the definition given by (15) we note that some effect of the wave is also included in  $|u_{*c}|$ .)

#### APPARENT ROUGHNESS

The concept of the apparent roughness  $k_{bc}$  is introduced in (47) by a direct analogy with fully developed rough turbulent unidirectional flow. For flow over a hydrodynamically rough bottom the separation around the individual roughness elements results in spatially varying pressure gradients in the flow. The presence of the pressure gradients causes the flow to feel a greater resistance, known as form drag, than that associated with the skin friction, i.e., that part of the resistance due to the Nikuradse roughness scale. In fact, what is happening in the case of form drag is that flow energy has been mechanically dissipated because of the generation of turbulent eddies in the separation process. In the same vein, for the coupled action of waves and currents the resulting larger boundary shear stress at the wall due to the presence of the wave creates a corresponding increase in the resistance felt by the steady flow above the wave boundary layer over that which is associated with the physical roughness  $k_b$ . This increased resistance manifests itself in the larger apparent roughness  $k_{bc}$  just as the increased shear stress due to form drag manifests itself in the physical bottom roughness  $k_b$ .

The physical bottom roughness and the apparent bottom roughness are explicitly related, since the steady current velocity

profile must be continuous across the wave boundary layer interface. Equating (44) and (47) at  $z = \delta_w$ , we have

$$\frac{|u_{*cw}|}{|u_{*c}|} = \frac{\ln(30\delta_w/k_b)}{\ln(30\delta_w/k_{bc})} \quad (48)$$

By definition the left-hand side of (48) is always greater than 1, and thus the apparent roughness  $k_{bc}$  is always greater than  $k_b$ , the physical bottom roughness.

Rearranging (48) with the aid of (38) and noting that  $|A_b| = |u_b|/\omega$ , the ratio of the apparent bottom roughness to the physical bottom roughness is found to be

$$\frac{k_{bc}}{k_b} = \left[ 24 \frac{|u_{*cw}|}{|u_b|} \left( \frac{|A_b|}{k_b} \right) \right]^\beta \quad (49)$$

where

$$\beta = \left( 1 - \frac{|u_{*c}|}{|u_b|} \frac{|u_b|}{|u_{*cw}|} \right)$$

The value of  $k_{bc}/k_b$  can be determined from (49) for specified values of  $|A_b|/k_b$  and  $\phi_c$  provided the wave current friction factor  $f_{cw}$  and the corresponding value of the velocity ratio  $|u_{*c}|/|u_b|$  are known. (The determination of these latter two parameters is treated in the following sections.) The variation of  $k_{bc}/k_b$  with  $|u_{*c}|/|u_b|$  for constant values of  $k_b/|A_b|$  is shown in Figure 3 for the case of codirectional flow, i.e.,  $\phi_c = 0^\circ$ . As  $\phi_c$  increases from  $0^\circ$  to  $90^\circ$ , the value of  $k_{bc}/k_b$  will decrease for constant values of  $|u_{*c}|/|u_b|$  and  $k_b/|A_b|$ . Comparison of the values of  $k_{bc}/k_b$  for  $\phi_c = 90^\circ$ , shown in Table 1 with the corresponding values in Figure 3, provides some feel for the behavior of the apparent roughness with angle. Thus according to (49), some influence of the wave on the current will always be present, but, as is expected, this influence diminishes as the current speed becomes large in relation to the wave orbital speed, i.e.,  $|u_{*c}|/|u_b|$  becomes large, and as the angle between the wave and current increases. For large values of the current relative to the wave  $|u_{*c}|/|u_b| > 1.0$ , the effect of the wave is significantly reduced for angles greater than  $45^\circ$ .

It is important to note that for small values of  $|u_{*c}|/|u_b|$ , in the range less than 0.25, the apparent roughness is considerably larger than the physical bottom roughness. For many conditions of interest on the shelf this is an important range of relative wave and current magnitudes. We also point out that the ratio  $k_{bc}/k_b$  is highly dependent on the order of magnitude of the relative roughness  $k_b/|A_b|$ . More discussion will be given to these observations in the concluding remarks.

Recent studies of nearshore currents by *Scott and Csanady* [1976] and *Forristall et al.* [1977] lend strong qualitative support to the concept of an apparent bottom roughness, as introduced here. Estimates by Scott and Csanady of bottom friction over a sand bed in water 32 m deep along the Long Island coast yielded a drag coefficient of  $8 \times 10^{-3}$ . This drag coefficient was found by Scott and Csanady to correspond to a calculated value of  $k_b$  equal to 69 cm based on the velocity at about 2 m above the bottom. The analysis of *Scott and Csanady* [1976] is based on current meter data that were averaged over tidal periods corresponding to wind stress events. Unfortunately, no direct wave measurements are available for those periods. However, on the basis of the wind stress events it is quite reasonable to state that significant wave motion was present for extended time periods during their study. This was confirmed by J. T. Scott (personal communication, 1977).

*Forristall et al.* [1977] analyzed measurements of waves and current velocities at three heights in the water column made during tropical storm Delia in the Gulf of Mexico in water

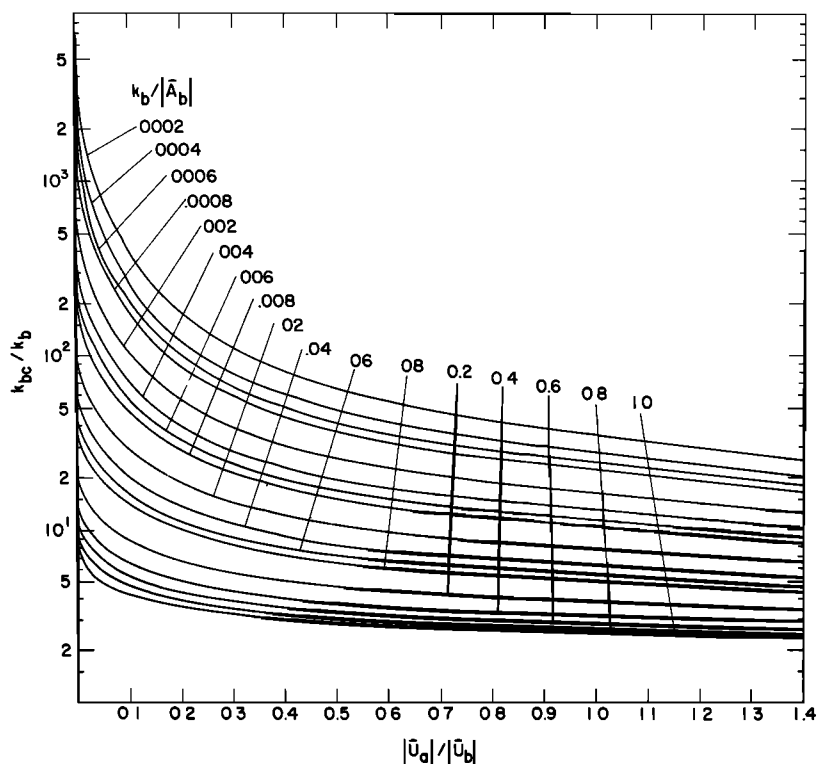


Fig. 3. Ratio of apparent bottom roughness  $k_{bc}$  to the physical bottom roughness  $k_b$  for codirectional flow, (49).

approximately 21 m deep. Maximum current speeds greater than 3 kn (1.5 m/s) at 2 m above the bottom along with wave heights up to 24 feet (7.3 m) were recorded. Using a simple logarithmic velocity profile model, Forristall et al. determined bottom roughnesses as high as 6 m over a mud bottom. Because of the lack of detailed information about the wave conditions and boundary geometry it is not possible to give an exact comparison between the model presented here and the measurements of Scott and Csanady [1976] and Forristall et al. [1977]. It is tempting to make at least a qualitative comparison. An order of magnitude estimate of the physical bottom roughness  $k_b$  may be made for the Scott and Csanady study, assuming that wave-formed ripples were present. Taking the maximum ripple steepness, i.e., height to length ratio, as 0.15 and the length as 1.5 times the excursion amplitude  $|A_b|$  [Dingler, 1974], we can obtain a reasonable estimate of the relative roughness,  $k_b/|A_b| \approx 0.5$ , upon assuming that  $k_b$  is approximately twice the ripple height [Grant, 1978]. In the case of the Forristall study, the presence of a mud bottom makes the estimate of  $k_b$  somewhat more difficult, but considering the high bed load transport rates, a reasonable value for  $k_b$  would be of the order of 2 cm.

Estimates of the wave conditions for each study are given in Table 2 (these estimates are based on personal communication with the investigators) along with other information necessary in order to use the theory presented here. The details of the calculation procedure are given in the discussion section be-

low. The results shown in Table 2 demonstrate that the roughness values predicted by the simple theory presented here are quite reasonable in light of the field measurement cited. Two different sets of values for the boundary shear stress and wave characteristics are presented for the Scott and Csanady case to illustrate that the roughness scale predicted is consistent with the likely range of wave and current conditions. In fact, exact agreement between the experimental value of the roughness and that predicted by the theory is possible by choosing the correct combination of wave height, period, and boundary shear stress. Clearly, such exact agreement would be fortuitous, and only typical magnitudes are used here.

It is interesting to note that even though Scott and Csanady [1976] and Forristall et al. [1977] use different analysis techniques, they arrive at similar observations of large bottom roughnesses. Both sets of investigators indicate that unsteady effects in the flow may possibly be the cause of their observations but do not undertake any analysis of the influence of the wave motion. Finally, we note that the range of wave and current conditions covered by the two studies would be expected to go from large waves and relatively small currents to waves and currents of similar magnitude as observed by G. Z. Forristall (personal communication, 1978) at the height of the storm. Thus these observations indicate the important influence of waves on currents over the wide range of conditions to be expected in the coastal zone.

#### DETERMINATION OF THE BOTTOM FRICTION

In order to use the theory presented here, the remaining task of determining the wave-current friction factor must be addressed. In a fashion analogous to the definition of the wave friction factor used by Jonsson [1966] we defined the wave current friction factor  $f_{cw}$  by relating the maximum bottom shear stress to the maximum velocity due to the wave and current in (19). Thus

TABLE 1. Values of  $k_{bc}/k_b$  for  $\phi_c = 90^\circ$

$k_b/ A_b $	$ u_a / u_b $				
	0.025	0.1	0.6	1.0	1.2
0.2	15.32	10.88	3.32	2.09	1.81
0.0002	2206.00	717.00	26.29	7.28	2.91

TABLE 2. Comparison With Field Observations

$\phi_c$ , deg	Wave Height, m	Wave Period, s	Water Depth, m	$ \mathbf{u}_{*c} ^2$ , $\text{cm}^2/\text{s}^2$	$k_b/ A_b $	$k_{bc}$ , Field, cm	$k_{bc}$ , Equation (49), cm
<i>Scott and Csanady</i>							
0	2	7	32	1	0.5	69	47
75	1	10	32	1	0.5	69	89
<i>Forristall et al.</i>							
0	3.66	8	20	25	0.02	30	29

The data of Forristall et al. refer to 0900 on September 4 [see Forristall et al., 1977, Figures 13 and 14].

$$|\tau_{b,max}|/\rho = |\mathbf{u}_{*cw}|^2 = \frac{1}{2} f_{cw} \alpha |\mathbf{u}_b|^2 \quad (50)$$

Since the maximum bottom shear stress is due to both the steady component and the unsteady component of the total motion, the magnitude of the vector sum of the maximum shear stress due to the wave,  $\tau_{w,max}$ , and the current  $\tau_c$  is equated to (50), giving

$$\rho^{-1} |\tau_c + \tau_{w,max}| = |\mathbf{u}_{*cw}|^2 \quad (51)$$

We emphasize that (50) represents the addition of a stress component associated with the unsteady motion and a stress component associated with the steady motion of the total enhanced motion due to the combined presence of a wave and a current which are coupled in a nonlinear fashion. These components result from the partitioning discussed previously; (50) does not represent the addition of the boundary stress associated with a pure wave plus that associated with a pure current.

In (51) the maximum shear stress associated with the wave can be expressed using the eddy viscosity as

$$\frac{\tau_{w,max}}{\rho} = |\mathbf{u}_{*w,max}| |\mathbf{u}_{*w,max}| = \lim_{z \rightarrow 0} \left[ \kappa |\mathbf{u}_{*cw}| z \left( \frac{\partial \mathbf{u}_w}{\partial z} \right)_{max} \right] \quad (52)$$

where  $\mathbf{u}_w$  is given by (36) and  $|\mathbf{u}_{*cw}|$  is given by (21).

For a pure wave motion, the use of an eddy viscosity based on the maximum values of the shear velocity such as that used

in (52) leads to a sine-squared variation in the shear stress with the free stream velocity (with a phase shift) (e.g., GM). This is in reasonable agreement with observations.

Introducing (36) into (52) and taking the limit, the magnitude of the maximum wave shear velocity squared at the bed is

$$|\mathbf{u}_{*w,max}|^2 = \kappa |\mathbf{u}_{*cw}| |\mathbf{u}_b| \zeta_0^{1/2} \left\{ \frac{1}{2\zeta_0^{1/2}} \frac{1}{(\text{Ker}^2 2\zeta_0^{1/2} + \text{Kei}^2 2\zeta_0^{1/2})^{1/2}} \right\} \quad (53)$$

Rewriting the expression for  $\zeta_0$  given by (31) with the use of (21) and noting  $|A_b| = |\mathbf{u}_b|/\omega$ , (53) may be rewritten and substituted into (51) along with the expressions for  $|\mathbf{u}_{*c}|^2$  and  $|\mathbf{u}_{*cw}|^2$  given by (15) and (50), respectively. After some algebraic manipulation the resulting general equation for the wave current friction factor becomes

$$\left[ 0.097 \left( \frac{k_b}{|A_b|} \right)^{1/2} \frac{K}{f_{cw}^{3/4}} \right]^2 + 2 \left[ (0.097) \left( \frac{k_b}{|A_b|} \right)^{1/2} \frac{K}{f_{cw}^{3/4}} \right] \left[ \frac{V_2}{2\alpha^{1/4}} \right] \cos \bar{\phi}_c = \frac{\alpha^{3/4}}{4} - \frac{V_2^2}{4\alpha^{1/2}} \quad (54)$$

where the term in braces in (53) has been replaced by  $K$ , i.e.,

$$K = \frac{1}{2\zeta_0^{1/2}} \frac{1}{(\text{Ker}^2 2\zeta_0^{1/2} + \text{Kei}^2 2\zeta_0^{1/2})^{1/2}} \quad (55)$$

In carrying out the indicated vector addition in (51) the maximum wave shear stress is assumed to act in the direction of wave propagation, whereas the time-averaged current shear stress is assumed to act in the direction of the current,  $\bar{\phi}_c$ , at the wave boundary layer interface. The relationship between  $\phi_c$  and  $\bar{\phi}_c$  was given in (17).

An example of the behavior of the wave-current friction factor governed by (54) is shown graphically in Figure 4 as a function of the parameters  $k_b/|A_b|$  and  $|\mathbf{u}_c|/|\mathbf{u}_b|$  and for values of  $\phi_c$  equal to  $0^\circ$  and  $90^\circ$ . For small values of  $|\mathbf{u}_c|/|\mathbf{u}_b|$  the value of  $f_{cw}$  is almost independent of the angle  $\phi_c$ ; numerical calculations show that for  $\phi_c < 60^\circ$  the codirectional flow solution adequately determines  $f_{cw}$ . In the limiting case of a pure wave motion, (54) shows excellent agreement with determinations of the wave friction factor based on Jonsson and Carlsson's [1976] experiments in an oscillatory wave boundary layer (e.g., GM).

DISCUSSION

The theoretical model described in this paper is easily programmed on a computer, and few iterations are required for solutions. The wave friction factor  $f_{cw}$  and the apparent roughness  $k_{bc}$  must be determined in order to find the flow kinemat-

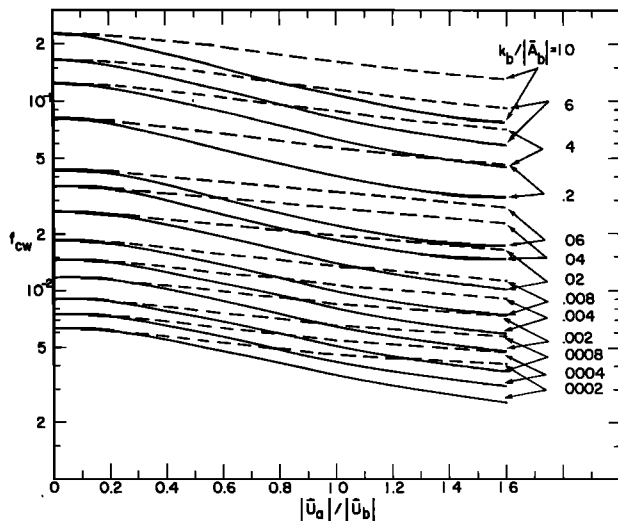


Fig. 4. Wave-current friction factor for codirectional flow,  $\phi_c = 0^\circ$  (solid lines), and transdirectional flow,  $\phi_c = 90^\circ$  (dashed lines), (54). (For  $\phi_c < 60^\circ$ , use solid line; for  $\phi_c > 60^\circ$ , interpolate.)

ics as well as the flow dynamics associated with the combined wave and current motion. In the preceding developments the behavior of these two parameters was given as a function of the relative roughness  $k_b/|A_b|$ , the velocity ratio  $|u_a|/|u_b|$ , and the current angle  $\phi_c$ . The latter two parameters are a priori unknown for reasons previously discussed and are found as part of the solution to the wave and current problem.

The determination of the parameters  $|u_a|/|u_b|$  and  $\phi_c$  is straightforward. We must first define a set of characteristic wave and current parameters. The current is characterized by its magnitude  $|u_{cr}|$  at a specified height above the bottom,  $z_r$ , and by an angle  $\bar{\phi}_c$  to the wave direction. The wave characteristics are represented by the near-bottom orbital wave velocity  $|u_b|$  and excursion amplitude  $|A_b|$ . In addition, an estimate of the physical bottom roughness  $k_b$  is required to characterize the fluid-sediment interaction. Thus four parameters, given in dimensionless form as

$$\frac{z_r}{k_b} \quad \frac{|u_{cr}|}{|u_b|} \quad \frac{k_b}{|A_b|} \quad \bar{\phi}_c \quad (56)$$

result. From these four quantities an iterative procedure is adopted to solve for the terms  $\phi_c$ ,  $|u_a|/|u_b|$ ,  $f_{cw}$ , and  $k_{bc}/k_b$  needed to calculate the bottom shear stress and velocity yield. The calculation procedure consists of first estimating a value of  $|u_a|/|u_b|$  along with a value of  $\phi_c$ . Using these two estimated values and the values of  $k_b/|A_b|$  and  $\bar{\phi}_c$ , given by (56),  $f_{cw}$  may be calculated from (54), and  $k_{bc}/k_b$  may then be found from (49). (Note that  $f_{cw}$  and  $k_{bc}/k_b$  can also be found graphically from Figures 4 and 3, respectively.) However, the solution is not yet closed. The specified magnitude of the current  $|u_{cr}|$  at a height  $z_r$  above the wave boundary layer is given by (47) with  $z = z_r$ , and hence the value of  $k_{bc}/k_b$  found from solving (47) must match the value calculated by using the assumed values of  $|u_a|/|u_b|$  and  $\phi_c$ . An iterative procedure is required until the value of  $k_{bc}/k_b$ , calculated from (49) by using the assumed values of  $|u_a|/|u_b|$  and  $\phi_c$ , matches the value calculated by using (47). As an alternative to (56) the first two parameters may be replaced by the magnitude of the boundary shear velocity due to the steady current, written in dimensionless form as  $|u_{*c}|/|u_b|$ . An iterative procedure is then adopted so that the calculated value of  $|u_{*c}|$  from the square root of (15) matches the specified value. The complete details of the iterative procedure required for the stress and velocity calculations are too long to be presented here, and the reader is referred to GM for a thorough discussion. The theory may also be used for hand calculations. A plot of  $V_2$  versus  $\phi_c$  for discrete values of  $|u_a|/|u_b|$  is provided in Figure 1 for this purpose.

For many cases of interest to sediment transport and circulation models on the inner continental shelf the ratio  $|u_a|/|u_b|$  is small. This is a convenient result, since for these conditions, i.e.,  $|u_a|/|u_b| < 0.25$ , the procedure to calculate the shear stress and velocity profiles is greatly simplified. Small current approximations for  $V_2$  and  $\bar{\phi}_c$  given by (16) and (18), respectively, may then be used.

The ability to carry out accurate calculations of the bottom shear stress under combined waves and currents is obviously important to sediment transport prediction. The transport of sediment as bed load is generally related to the skin friction component of the total shear stress at the bed. Procedures have been devised in unidirectional flow by *Einstein* [1950], *Smith and McLean* [1977], and others to find the skin friction component of the total stress. *Madsen and Grant* [1976, 1977] have shown that in the case of sediment transport under waves the

skin friction component of a bed shear stress may be evaluated by using the sand grain diameter as the appropriate roughness in determining the wave friction factor in the shear stress equation. To calculate the skin friction for the case of combined waves and currents, it is reasonable to adopt an approach similar to that used by *Madsen and Grant* for pure waves. However, the total shear stress given by (8) must first be evaluated by using the physical bottom roughness  $k_b$  as the appropriate roughness; i.e., a value of  $|u_a|$  must be found. Verification of such an approach for combined waves and currents awaits experimental evidence. When multiple roughness scales are present, assuming they are small enough that significant wave scattering does not occur, an approach similar to that suggested by *Smith and McLean* [1977] would also have to be considered.

The influence of the wave motions on the bed can cause significant quantities of sediment to be suspended above the bed, where it is then transported with nearly the horizontal component of the current velocity. Accurate knowledge of the current velocity above the bed is clearly needed to calculate the suspended load transport. The theory presented here indicates that the current above the wave boundary layer will feel a greater resistance due to the presence of the wave. This increased resistance will result in a steepening of the velocity profile associated with the wave-influenced current over that of a current with no wave influence. Since the suspended concentration is greatest close to the bed where the current profile is reduced the most, it is obvious that the ability to account for the wave influence on the current velocity profile is critical to the successful modeling of suspended load transport.

A more quantitative measure of the influence of the wave on the current is presented in Table 3. Values of the depth-averaged current calculated by including the influence of the wave, using the present theory and neglecting it, are given for the values of the reference parameters in (56) indicated in the table. Values of  $k_b$  were estimated as described above. It is seen that for the conditions in the table, up to a 33% reduction in the depth-averaged velocity would occur by accounting for the influence of the wave. From the consideration of suspended sediment transport, accurate knowledge of the velocity near the bed is most important; neglecting the influence of the wave would result in overprediction of the current velocity half a meter above the bed by as much as a factor of 2 in the example cited. The implications of this very idealized calculation extend beyond considerations of only sediment transport and show the importance of the inclusion of wave influence in coastal circulation models. These results also point out the importance of monitoring storm events for the successful calibration of circulation models, since roughness values determined during periods of calm weather would be expected to be significantly smaller than those found during storm conditions.

#### CONCLUDING REMARKS

Clearly, the mean shear stress (mean in the Reynolds sense only) given by (8) never actually moves any sediment. In the case of a rough bed the individual sediment grains are reacting to the action of turbulent eddies which 'kick' them loose from the bed (we physically picture a momentary pressure differential across the grain). The nature of these turbulent eddies is random, as is the stability of the individual sediment grains. However, from a deterministic viewpoint the empirical relationship between the local mean shear stress and the local transport of sediment seems to be a valid indicator of the average transport conditions. More sophistication in this con-

TABLE 3. Comparison of Mean Velocities With and Without the Effect of Waves

$z_r/k_b$	$ \mathbf{u}_c / \mathbf{u}_b $	$k_b/ \mathbf{A}_b $	$\phi_c$ , deg	$ \mathbf{u}_a / \mathbf{u}_b $	$k_{bc}/k_b$	$\bar{u}/ \mathbf{u}_b $	$ \mathbf{u}_c / \mathbf{u}_b $
5	0.74	0.2	0	0.19	7.0	1.98	1.51
5	0.45	0.2	0	0.085	9.5	1.33	0.96
5	0.18	0.2	0	0.018	14.0	0.61	0.42

Water depth is 32 m,  $T = 10$  s, wave height is 2 m,  $z_r = 0.5$  m,  $|\mathbf{A}_b| = 0.5$  m,  $\bar{u}/|\mathbf{u}_b| = (|\mathbf{u}_c|/|\mathbf{u}_b|)(1/\kappa) \ln(11.04h/k_b)$ , and  $\bar{u}_c/|\mathbf{u}_b| = (|\mathbf{u}_c|/|\mathbf{u}_b|)(1/\kappa) \ln(11.04h/k_{bc})$ .

cept does not seem justifiable until quantitative knowledge of the structure of turbulent boundary layers over roughened beds in oscillatory flow is available.

The use of an eddy viscosity in the model here is another direct consequence of our lack of detailed knowledge of the structure of turbulent boundary layers. In order to treat the problem of combined waves and currents interacting with a rough bottom in a mathematical form, a simple linearly varying eddy viscosity model was used in the present theory. We pointed out that in many geophysical flows the simple mixing length arguments behind such models are not valid because of multiple length scales involved in the flow. However, close to the bed, where the proper length scale is the bed roughness, i.e., wave-formed ripples, the model is expected to be reasonable. The good agreement cited with laboratory experiments for pure waves and the reasonable nature of the results of the model for predictions of the apparent roughness are put forth as support for this claim. Higher in the flow, where other length scales may be involved, the appropriate value of the characteristic shear velocity should reflect this in much the same manner as the two boundary layer regions in this model reflect the scales of wave and current influence. From (22) and (23) it is clear that a discontinuity exists in the eddy viscosity profile across the wave boundary layer interface. This is of no consequence to the physics of the model presented here; in any case, it is easily treated.

One major obstacle encountered in developing the theory presented here is the lack of data which can be used to test the theory's quantitative ability. The paucity of data is quite understandable when one considers the difficulties involved in making the near-bottom velocity measurements required to obtain data on combined wave and current flows. Current meters are required which have accurate zero points, have rapid sampling ability, and are capable of responding accurately in reversing flows. The scale of the wave boundary layer, approximately 5–10 cm for typical wind-driven waves, requires the use of velocity-measuring devices with small sampling volumes. Knowledge of the bed geometry is also required. However, with our present state of knowledge it is unlikely that we can accurately specify the associated physical bottom roughness within more than a factor of 2 or 3.

In the field, except under the most idealized conditions, the complications involved in making the physical measurement will be equally matched by the complications involved in interpreting the data unless great care is taken in setting up the experiment and making the measurements. The problems of a movable bed, a random sea, and the background level of turbulence contained in the current due to vorticity introduced, for example, by larger-scale topography are not well understood at this time. The present theory is an attempt at providing a stepping stone to help plan and interpret such measurements. As more data become available, the assumptions made in the model may be more carefully investigated, and the theory can be improved.

In summary, the theory presented here identifies a set of

physically meaningful parameters which may be used to quantify combined wave and current interaction with a rough bottom. The theory shows that when waves and currents exist jointly in a region, the shear stresses identified with the wave and the current are altered because of the nature of the turbulence generated by the wave-current interaction at the bed and are different from the stresses expected in the case of pure waves or currents. The net result is that the current in the region above the wave boundary layer feels a greater resistance than that associated with the physical bottom roughness. This greater resistance is introduced in the model through the concept of an apparent bottom roughness which reflects the characteristics of the wave boundary layer. The theory also gives solutions for the flow kinematics both inside and outside the wave boundary layer. The procedure for use of the model developed is briefly outlined, and the reader is referred to a more detailed discussion by GM. (The initial work presented by Grant [1977] and Grant and Madsen [1978] has been modified as described by Grant [1978].

*Acknowledgments.* The research presented in this paper was initiated as part of a doctoral dissertation of William D. Grant, prepared under the guidance of Ole S. Madsen at Ralph M. Parsons Laboratory, Massachusetts Institute of Technology. The initial research was sponsored by the Marine Geology and Geophysics Laboratory, NOAA/AOML, as part of Project Instep (Inner Shelf Sediment Transport Experiment) under contract 03-6-022-35220. The first author expresses his gratitude to the Mellon Foundation at Woods Hole Oceanographic Institution, who provided additional funds to continue the work. Woods Hole Oceanographic Institution contribution 4250.

#### REFERENCES

- Abramowitz, M., and I. A. Stegun, *Handbook of Mathematical Functions, Appl. Math. Ser.*, no. 55, pp. 379–509, National Bureau of Standards, Washington, D. C., 1972.
- Butman, B., M. Noble, and D. W. Folger, Observations of bottom current and bottom sediment movement on the mid-Atlantic continental shelf (abstract), *Eos Trans. AGU*, 58(6), 408, 1977.
- Coleman, H. W., R. J. Moffat, and W. M. Kays, The accelerated fully rough turbulent boundary layer, *J. Fluid Mech.*, 82, 507–528, 1977.
- Dingler, J. R., Wave formed ripple in nearshore sands, Ph.D. thesis, 136 pp., Scripps Inst. of Oceanogr., La Jolla, Calif., 1974.
- Einstein, H. A., The bed-load function for sediment transportation in open channel flows, *Tech. Bull. 1026*, U.S. Dep. of Agr., Washington, D. C., Sept. 1950.
- Forristall, G. Z., R. C. Hamilton, and V. T. Cardone, Continental shelf currents in tropical storm Delia: Observations and theory, *J. Phys. Oceanogr.*, 7(4), 532–536, 1977.
- Grant, W. D., Bottom friction under waves in the presence of a weak current: Its relationship to coastal sediment transport, Sc.D. thesis, 275 pp., Mass. Inst. of Technol., Cambridge, 1977.
- Grant, W. D. and O. S. Madsen, Bottom friction under waves in the presence of a weak current, *NOAA Tech. Rep. ERL-MESA*, 150 pp., 1978.
- Grant, W. D., Notes on bottom friction under combined waves and currents, internal report, Woods Hole Oceanogr. Inst., Woods Hole, Mass., 1978.
- Hildebrand, F., *Calculus for Applications*, 646 pp., Prentice-Hall, Englewood Cliffs, N. J., 1965.
- Horikawa, K., and A. Watanabe, Laboratory study of oscillatory boundary layer flow, *Proc. Coastal Eng. Conf. 11th*, chap. 29, 467–486, 1968.

- Jonsson, I. G., Wave boundary layers and friction factors, *Proc. Coastal Eng. Conf. 10th, I*, 127-148, 1966.
- Jonsson, I. G., and N. A. Carlsen, Experimental and theoretical investigations in an oscillatory turbulent boundary layer, *J. Hydraul. Res.*, 14(1), 45-60, 1976.
- Kajiura, K., On the bottom friction in an oscillatory current, *Bull. Earthquake Res. Inst.*, 42, 147-174, 1964.
- Kajiura, K., A model of the bottom boundary layer in water waves, *Bull. Earthquake Res. Inst.*, 46, 75-123, 1968.
- Komar, P. D., R. H. Neudeck, and L. D. Kulm, Observations and significance of deep-water oscillatory ripple marks on the Oregon continental shelf, in *Shelf Sediment Transport*, edited by D. J. P. Swift, D. B. Duane, and O. H. Pilkey, 656 pp., Hutchinson and Ross, Stroudsburg, Pa., 1972.
- Madsen, O. S., Wave climate of the continental margin: Elements of its mathematical description, in *Marine Sediment Transport and Environment*, edited by D. J. Stanley and D. J. P. Swift, 602 pp., Wiley-Interscience, New York, 1976.
- Madsen, O. S., and W. D. Grant, The threshold of sediment movement under oscillatory water waves: A discussion, *J. Sediment. Petrology*, 45(2), 360-361, 1975.
- Madsen, O. S., and W. D. Grant, Sediment transport in the coastal environment, *Rep. 209*, 105 pp., Ralph M. Parsons Lab. for Water Resour. and Hydrodyn., Dep. of Civil Eng., Mass. Inst. of Technol., Cambridge, 1976.
- Madsen, O. S., and W. D. Grant, Quantitative description of sediment transport by waves, *Proc. Coastal Eng. Conf. 15th, II*, 1093-1112, 1977.
- Schlichting, H., *Boundary Layer Theory*, 4th ed., 647 pp., McGraw-Hill, New York, 1968.
- Scott, J. T., and G. T. Csanady, Nearshore currents off Long Island, *J. Geophys. Res.*, 81(30), 5401-5409, 1976.
- Smith, J. D., Modeling of sediment transport on continental shelves, in *The Sea*, vol. 6, Wiley-Interscience, New York, 1977.
- Smith, J. D., and S. R. McLean, Spatially averaged flow over a wavy surface, *J. Geophys. Res.*, 82(12), 1735-1746, 1977.

(Received April 27, 1978;  
revised December 5, 1978;  
accepted December 18, 1978.)